J. Am. Chem. Soc. 1987, 109, 7346-7352

Stabilities and Structures in Cluster Ions of Five-Membered Heterocyclic Compounds Containing O, N, and S Atoms

K. Hiraoka,*[†] H. Takimoto,[†] and S. Yamabe*[‡]

Contribution from the Faculty of Engineering, Yamanashi University, Takeda-4, Kofu 400, Japan, and Department of Chemistry, Nara University of Education, Takabatake-cho, Nara 630, Japan. *Received April 14, 1987*

Abstract: Clustering and hydration reactions of protonated and radical cations of heterocyclic compounds, e.g., furan, tetrahydrofuran, pyrrole, pyrrolidine, thiophene, and tetrahydrothiophene, have been studied using a pulsed electron beam mass spectrometer. The bond energies of proton-held dimer cations for furan, pyrrole, and thiophene are much smaller than those for tetrahydrofuran, pyrrolidine, and tetrahydrothiophene, respectively. This result suggests that not the heteroatoms but the α carbon atoms are protonated for furan, pyrrole, and thiophene. The hydrogen-bond site for the protonated furan and thiophene is calculated to be the unprotonated α hydrogen (C–H_α adjacent to the heteroatom) which is the most acidic one. On the other hand, the N–H hydrogen is the best hydrogen-bond site for the protonated pyrrole. It was found that the radical-cation dimers have greater bond energies than the proton-held dimer cations for furan and thiophene. This suggests that the bonds of the former have more covalent nature. Some unique reactions of $C_4H_4O^{\bullet+}$ and $C_4H_5O^+$ with a furan molecule were observed. With an increase of temperature, the ions with m/z which are the same as those for $(C_4H_4O)_2^{\bullet+}$ and $H^+(C_4H_4O)_2$ are found to be formed at the expense of $C_4H_4O^{\bullet+}$ and $C_4H_5O^+$ ions, respectively. It is suggested that the reactions observed are Diels–Alder-type condensation reactions.

Heterocyclic compounds play very important roles in many fields. Heterocyclic intermediates are being used more and more in synthesis as protecting groups, readily generated, and also readily removed. Furan, pyrrole, and thiophene are anticipated to be emitted into the atmosphere in significant amounts from fuel conversion facilities. In the field of biology, heterocyclic compounds are found everywhere. Carbohydrates are heterocyclic, so are chlorophyll and heme. Heterocycles form the sites of reaction in many enzymes and coenzymes. Heredity comes down, ultimately, to the particular sequence of attachment of a half-dozen heterocyclic rings to the long chains of nucleic acids.

So far, detailed and comprehensive studies on the ion–molecule reactions in gaseous heterocyclic compounds are rather scarce. McMahon[1] and Meot-Ner[2] measured relative stabilities of proton-bound dimers of a number of n-donor bases including tetrahydrofuran, dioxane, and tetrahydropyran. They confirmed the finding by Kebarle[3-6] that in proton-bound dimers $BH^+\cdots A$, a linear correlation exists between the bond dissociation energies, ΔH_D° and the difference, ΔPA, between the proton affinities of the proton donor B and the proton acceptor A. Further, Meot-Ner et al.[7] found that the bond energies of hydrates of protonated furan and pyrrole are substantially lower than the values expected on the basis of $-OH^+\cdots O$ and $-NH^+\cdots O$ type hydrogen bonds. They suggested that the protonation sites of furan and pyrrole are not the heteroatoms but the α carbons of the rings.

In the present work, we focus our attention on the heterocyclic compounds with five-membered rings containing oxygen, nitrogen, and sulfur, i.e., tetrahydrofuran, pyrrolidine, tetrahydrothiophene, furan, pyrrole, and thiophene, where the arrows represent the direction of the dipoles and the numerical numbers represent the values of the permanent dipole moments in debye units. We studied the ion–molecule reactions of these compounds in various respects, e.g., clustering and hydration reactions of protonated and radical cations of the molecules, and kinetic studies of ion–molecule reactions observed for these compounds. From these studies, fairly complete thermochemical and kinetic descriptions may be obtained for the processes involved.

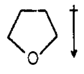

1.73 D
tetrahydrofuran

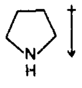

1.58 D
pyrrolidine

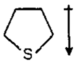

1.90 D
tetrahydrothiophene

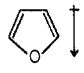

0.70 D
furan

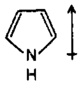

1.81 D
pyrrole

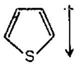

0.51 D
thiophene

It was found that clustering reactions observed at low temperature change into condensation reactions at high temperature in carbonium ion–H_2[8] and hydrocarbon system,[9,10] and in carbonium ion–HCN system.[11] In the present experiment, similar reactions in $C_4H_4O^{\bullet+}$–C_4H_4O and in $C_5H_5O^+$–C_4H_4O systems were also observed. These reactions are assigned to the Diels–Alder reactions.

Experimental Section

The measurements were made with a pulsed electron beam mass spectrometer which has been described previously.[12-14] Mixtures of heterocyclic compounds of interest in a carrier gas were prepared in a gas-handling system and allowed to flow into the ion source. Ionizing pulses of 2-keV electron beam initiated reaction sequences leading to the equilibria of interest. Ions escaping from the field-free ion source into an evacuated region were mass analyzed by a quadrupole mass spectrometer (ULVAC MSQ-400) and collected in a multichannel analyzer as a function of their arrival time after the electron pulse. The ion counts collected in a multichannel analyzer were transferred to a microcomputer, and time profiles of the ion counts were recorded on the x–y plotter.

[†] Yamanashi University.
[‡] Nara University of Education.

(1) Larson, J. W.; McMahon, T. B. *J. Am. Chem. Soc.* **1982**, *104*, 6255.
(2) Meot-Ner, M. *J. Am. Chem. Soc.* **1984**, *106*, 1257.
(3) Payzant, J. D.; Yamdagni, R.; Kebarle, P. *Can. J. Chem.* **1971**, *49*, 3308.
(4) Yamdagni, R.; Kebarle, P. *J. Am. Chem. Soc.* **1971**, *93*, 7139.
(5) Yamdagni, R.; Kebarle, P. *J. Am. Chem. Soc.* **1973**, *95*, 3504.
(6) Davidson, W. R.; Sunner, J.; Kebarle, P. *J. Am. Chem. Soc.* **1979**, *101*, 1675.
(7) Meot-Ner, M.; Ross, M. M.; Campana, J. E. *J. Am. Chem. Soc.* **1985**, *107*, 4839.
(8) Hiraoka, K.; Kebarle, P. *J. Am. Chem. Soc.* **1976**, *98*, 6119.
(9) Hiraoka, K.; Kebarle, P. *J. Chem. Phys.* **1975**, *63*, 394.
(10) Hiraoka, K.; Kebarle, P. *Can. J. Chem.* **1976**, *54*, 1739.
(11) Meot-Ner, M. *J. Am. Chem. Soc.* **1978**, *100*, 4694.
(12) Hiraoka, K.; Morise, K.; Shoda, T. *Int. J. Mass Spectrom. Ion Processes* **1985**, *67*, 11.
(13) Hiraoka, K.; Morise, K.; Nishijima, T.; Nakamura, S.; Nakazato, M.; Ohkuma, K. *Int. J. Mass Spectrom. Ion Processes* **1986**, *68*, 99.
(14) Hiraoka, K.; Takimoto, H.; Yamabe, S. *J. Phys. Chem.* **1986**, *90*, 5910.

0002-7863/87/1509-7346$01.50/0

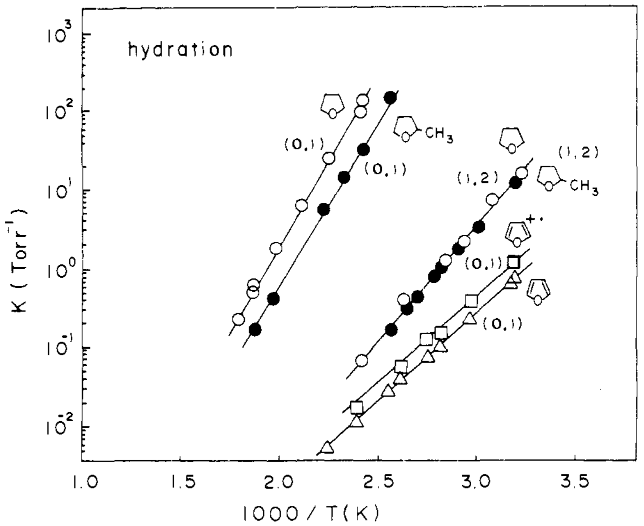

Figure 1. van't Hoff plots for the hydration reactions of protonated and radical cations for tetrahydrofuran (C_4H_8O), 2-methyltetrahydrofuran ($C_5H_{10}O$), and furan (C_4H_4O): (○) $C_4H_8OH^+(H_2O)_{n-1} + H_2O = C_4H_8OH^+(H_2O)_n$, (●) $C_5H_{10}OH^+(H_2O)_{n-1} + H_2O = C_5H_{10}OH^+(H_2O)_n$, (△) $C_4H_5O^+(H_2O)_{n-1} + H_2O = C_4H_5O^+(H_2O)_n$, (□) $C_4H_4O^{\cdot+}(H_2O)_{n-1} + H_2O = C_4H_4O^{\cdot+}(H_2O)_n$.

In the present study, equilibria for the following hydration and clustering reactions have been dealt with:

$$BH^+(H_2O)_{n-1} + H_2O = BH^+(H_2O)_n \tag{1}$$

$$B^{\cdot+}(H_2O)_{n-1} + H_2O = B^{\cdot+}(H_2O)_n \tag{2}$$

$$BH^+(B)_{n-1} + B = BH^+(B)_n \tag{3}$$

$$B^{\cdot+}(B)_{n-1} + B = B^{\cdot+}(B)_n \tag{4}$$

where the base B is a heterocyclic compound. In the measurements of the equilibria for reaction 1, a mixture of 0.001% B, 0.5–5% H_2O, and CH_4 was used as a reagent gas. The total pressure of the mixed gases was kept at ~4 torr. In the measurements of equilibria for reaction 2, a mixture of 0.01% B, 0.5–5% H_2O, 30% CS_2, and Ar was used as a reagent gas. With these conditions, $B^{\cdot+}$ is generated by the following sequence of chemical ionization processes:

$$Ar^{\cdot+} + CS_2 = CS_2^{\cdot+} + Ar \tag{5}$$

$$CS_2^{\cdot+} + B = B^{\cdot+} + CS_2 \tag{6}$$

The radical cations $B^{\cdot+}$ could be observed for tetrahydrothiophene, furan, pyrrole, and thiophene, but not for tetrahydrofuran and pyrrolidine. The short lifetimes of $B^{\cdot+}$ for the latter two compounds may be due to the rapid consumption of $B^{\cdot+}$ by reactions 7 and 8:

$$C_4H_8O^{\cdot+} + C_4H_8O = C_4H_8OH^+ + C_4H_7O \tag{7}$$

$$C_4H_8NH^{\cdot+} + C_4H_8NH = C_4H_8NH_2^+ + C_4H_8N \tag{8}$$

In the measurements of the equilibria for reaction 3, a mixture of 0.1–5% B, 30% C_6H_6, and CH_4 was used as a reagent gas. With these conditions, ions of heterocyclic compounds are generated by the following sequence of reactions:

$$CH_5^+ + C_6H_6 = C_6H_7^+ + CH_4 \tag{9}$$

$$C_2H_5^+ + C_6H_6 = C_6H_7^+ + C_2H_4 \tag{10}$$

$$C_6H_7^+ + B = BH^+ + C_6H_6 \tag{11}$$

The $C_6H_7^+$ ion generated by reactions 9 and 10 are known to be deactivated by collisions with methane before undergoing ring rupture.[15] In the measurements of equilibria for reaction 4, a mixture of 0.1–5% B, 30% CS_2, and Ar was used as a reagent gas. It was found that the observed equilibrium constants for reactions 3 and 4 are independent of the change of pressure of B for a range of more than one order of magnitude. This strongly suggests that the cyclic structures of B are preserved under the present experimental conditions.

The molecular orbital calculations using the STO-3G and 6-31G basis sets are carried out with the GAUSSIAN 80 program[16] so as to get information on the structure and the electron distribution of clusters. Since the sizes of the present clusters are large, the double-ζ-level MO calculation is difficult. The positional difference of the electron distributions is of central interest, and therefore the minimal-basis-set calculation is sufficiently informative for such comparison. For furan, the dipole moments calculated by seven methods are displayed in Table I. The double ζ (or double ζ plus polarization) overestimates the dipole moment.

Table I. Dipole Moments of Furan Calculated Using Seven Basis Sets

basis set	quality	dipole moment[a] (D)
STO-3G	minimal	0.43
STO-4G		1.21
3-21G	double-ζ	2.05
4-31G		2.15
6-31G		2.23
6-31G*	double-ζ plus polarization	2.39
6-31G**		2.37
exptl		0.70

[a] The experimental geometry of furan is adopted.

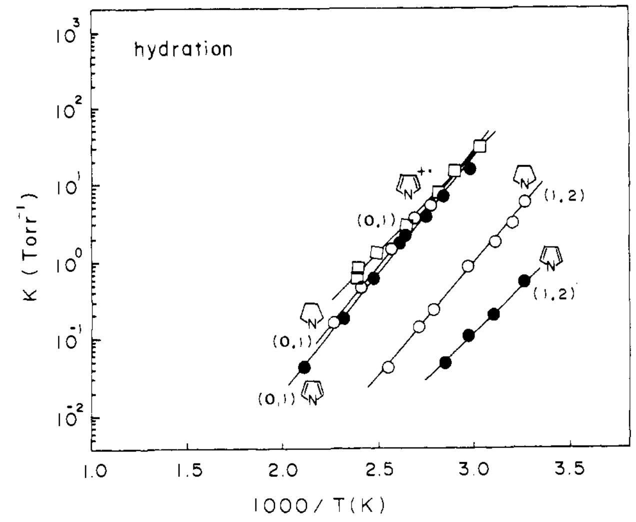

Figure 2. van't Hoff plots for the hydration reactions of protonated and radical cations for both pyrrolidine (C_4H_8NH) and pyrrole (C_4H_4NH): (○) $(C_4H_8NH_2^+(H_2O)_{n-1} + H_2O = C_4H_8NH_2^+(H_2O)_n$, (●) $C_4H_5NH^+(H_2O)_{n-1} + H_2O = C_4H_5NH^+(H_2O)_n$, (□) $C_4H_4NH^{\cdot+}(H_2O)_{n-1} + H_2O = C_4H_4NH^{\cdot+}(H_2O)_n$.

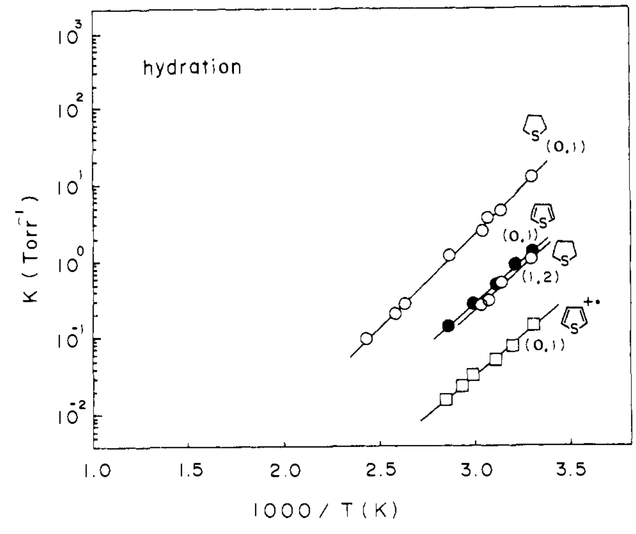

Figure 3. van't Hoff plots for the hydration reactions of protonated and radical cations for tetrahydrothiophene (C_4H_8S) and thiophene (C_4H_4S): (○) $C_4H_8SH^+(H_2O)_{n-1} + H_2O = C_4H_8SH^+(H_2O)_n$, (●) $C_4H_5S^+(H_2O)_{n-1} + H_2O = C_4H_5S^+(H_2O)_n$, (□) $C_4H_4S^{\cdot+}(H_2O)_{n-1} + H_2O = C_4H_4S^{\cdot+}(H_2O)_n$.

---

(15) Lias, S. G.; Ausloos, P. *J. Chem. Phys.* **1985**, *82*, 3613.

(16) Binkley, J. S.; Whiteside, R. A.; Krishnan, R.; Seeger, R.; DeFrees, D. J.; Schlegel, H. B.; Topiol, S.; Kahn, L. R.; Pople, J. A. GAUSSIAN 80: *QCPE* **1981**, *13* 406.

Table II. Thermochemical Data for the Hydration Reactions of Protonated Bases BH^+, $BH^+(H_2O)_{n-1} + H_2O = BH^+(CH_2O)_n$[a]

B	(0, 1)		(1, 2)	
	$-\Delta H°$	$-\Delta S°$	$-\Delta H°$	$-\Delta S°$
	19.8 21.8[b]	25.1 28.8[b]	13.1	24.0
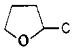	18.5	24.8	13.1	24.0
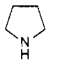	13.7	21.1	13.0	25.9
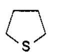	11.5	19.5	10.4	21.0
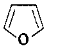	10.2	19.7		
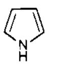	13.8	22.0	10.9	23.7
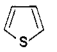	10.2	19.9		

[a] $-\Delta H°$ in kcal/mol, $-\Delta S°$ in cal/deg·mol, standard state 1 atm. [b] Reference 2.

Table III. Thermochemical Data for the Hydration Reactions of Radical Cations $B^{\cdot+}$, $B^{\cdot+}(H_2O)_{n-1} + H_2O = B^{\cdot+}(H_2O)_n$[a]

B^+	(0, 1)		(1,2)	
	$-\Delta H°$	$-\Delta S°$	$-\Delta H°$	$-\Delta S°$
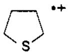	<10			
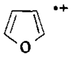	9.8	17.8		
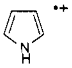	11.7	15.5	8.6	(15)[b]
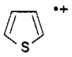	9.5	17.7		

[a] $-\Delta H°$ in kcal/mol, $-\Delta S°$ in cal/deg·mol, standard state 1 atm. [b] Entropy value assumed.

Rather, the minimal basis set is more acceptable to study the electronic distribution. However, for $C_4H_8SH^+(H_2O)_2$, the 6-31G basis set is used. This is because the potential curve of the proton transfer is reproduced incorrectly with STO-3G and correctly with 6-31G.

Results and Discussion

1. Hydration Reactions of Protonated and Radical Cations of Heterocyclic Compounds. Figures 1–3 show the van't Hoff plots for the hydration reactions 1 and 2 for B = tetrahydrofuran, 2-methyltetrahydrofuran, furan, pyrrolidine, pyrrole, tetrahydrothiophene, and thiophene. Thermochemical data obtained from these van't Hoff plots are summarized in Tables II and III.

The bond energies of the clusters $BH^+(H_2O)$ decrease in the order, tetrahydrofuran > pyrrolidine > tetrahydrothiophene. This is in the same order of the electronegativities for O (3.5), N (3.0), and S (2.5) atoms. The positive charge density on the protic hydrogen of the protonated base BH^+ decreases with decrease of the electronegativity of the heteroatom because of charge delocalization. This effect qualitatively explains the order of the observed bond energies.

A rapid decrease in the values of $-\Delta H°_{n-1,n}$ for tetrahydrofuran is observed between $n = 1$ and 2. This is reasonable since the monohydrated cation $C_4H_8OH^+\cdots OH_2$ forms the first filled-shell structure and the second H_2O molecule must interact with the cluster from outside of the first shell. On the other hand, the protonated pyrrolidine $C_4H_8NH_2^+$ possesses two protic hydrogens, and dihydrated cation $C_4H_8NH_2^+(H_2O)_2$ forms the first filled-shell structure. This explains the small decrease in the values between $-\Delta H°_{0,1}$ and $-\Delta H°_{1,2}$. It is interesting to note that the values of $-\Delta H°_{0,1}$ and $-\Delta H°_{1,2}$ for tetrahydrothiophene are quite close although the protonated tetrahydrothiophene is a monoprotic acid. When tetrahydrothiophene is protonated, the cationic nature is transmitted effectively into the ring. Values in parentheses are Mulliken atom populations.

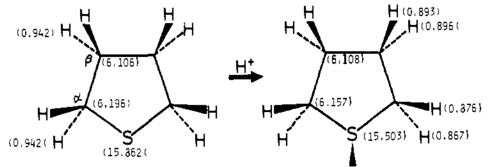

A MO calculation reveals that the α hydrogen is the most acidic one (0.867) in tetrahydrothiophene. In this species, however, the best hydrogen-bond site is not the C_α–H but the S–H hydrogen. The 6-31G calculated binding energy, 11 kcal/mol, of the C_α-H$\cdots OH_2$ bond is much smaller than that, 20 kcal/mol, of the S—H$\cdots OH_2$ bond. This energy difference demonstrates that a water molecule is bound more strongly to the S–H hydrogen than to the C_α–H site. It may be considered that in this cluster the role of the charge transfer (CT) from the lone-pair orbital of the water oxygen atom to the S–H antibonding orbital is more important than that of the Coulombic attraction. The average S–H binding energy (83 kcal/mol) is smaller than the O–H energy (111 kcal/mol), and the hard acid, proton, prefers to be pulled by the hard-base oxygen atom rather than the soft-base sulfur atom. In fact, the 6-31G partial optimization gives the elongation of the S–H bond (1.35 → 1.40 Å) through the hydration. The small difference of the enthalpy change between (0, 1) and (1, 2) is attributable to the enhancement effect of the cationic nature. That is, the first water molecule is polarized effectively by the clustering, O (8.87) and H (0.53) relative to O (8.80) and H (0.60) of the free water molecule. The second water molecule is bound to the first one. An alternative model of $n = 2$, S—H$\cdots OH_2$ plus C_α—H$\cdots OH_2$, is calculated to be 8.6 kcal/mol (6-31G) less stable than the model in the figure.

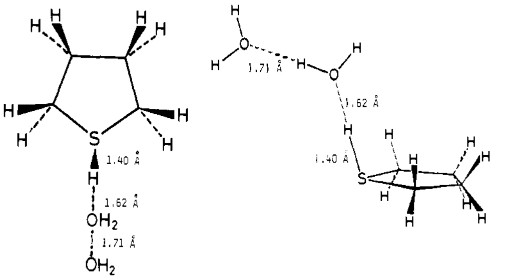

In the measurement of hydration reaction 2 of $C_4H_8S^{\cdot+}$, the hydrated ion $C_4H_8S^{\cdot+}(H_2O)$ was found to decrease more gradually than $C_4H_8S^{\cdot+}$ after the ionizing electron pulse, probably because of the buildup of the impurity ion whose m/z is equal to that of $C_4H_8S^{\cdot+}(H_2O)$. Thus the equilibria for this reaction could not be observed. By measuring ion intensities of $C_4H_8S^{\cdot+}$ and $C_4H_8S^{\cdot+}(H_2O)$ right after the ionizing electron pulse, the upper limit of the equilibrium constants may be given. The bond energy ($-\Delta H°$) of the cluster $C_4H_8S^{\cdot+}(H_2O)$ could only be estimated to be less than 10 kcal/mol, assuming $-\Delta S° = 20$ cal/mol·K for this reaction.

The bond energy of the cluster of the protonated furan with H_2O is almost a half that of the protonated tetrahydrofuran with H_2O. If the O atom of C_4H_4O were protonated, the bond energy of $C_4H_4OH^+\cdots OH_2$ would be more or less the same as that of $C_4H_8OH^+\cdots OH_2$. The much lower bond energy of the hydrated cluster $H^+(C_4H_4O)(H_2O)$ suggests that the most favorable protonation site of the furan molecule is not the O atom but the ring as was already pointed out by Meot-Ner et al.[7] The protonation site on the ring is most likely the α-carbon atom. The selectivity of the protonation site will be discussed in section 3A. The hydrogen-bond site is calculated to be the unprotonated α (called α') hydrogen which is the most acidic (0.802) one. The acidity comes naturally from the oxygen atom adjacent to the α' C–H bond.

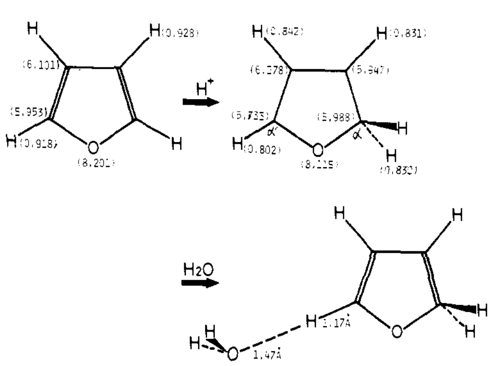

(12)

For pyrrole, similarly, the protonation site is not the N atom but the α carbon on the ring. When protonated, the N–H hydrogen becomes very acidic as is represented by eq 13. The presence of the (0.697) proton may be the reason why $-\Delta H^\circ_{0,1}$ for pyrrole is greater than those for furan and thiophene.

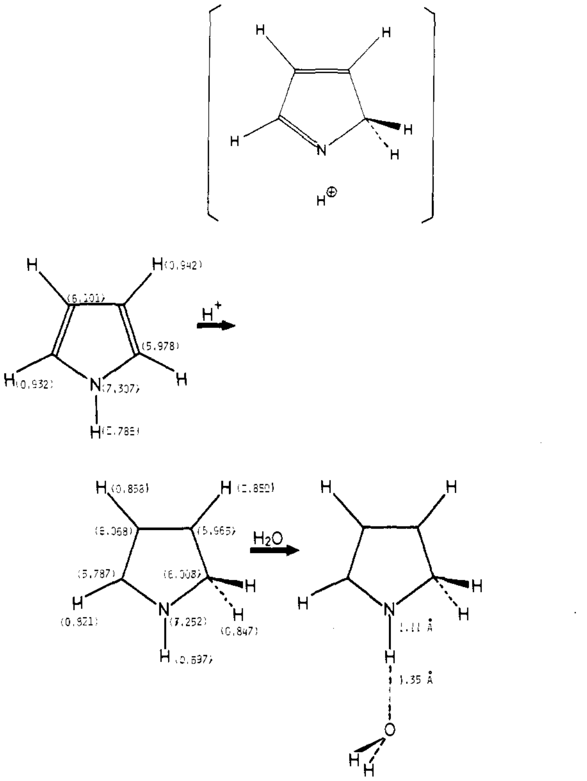

(13)

The most favorable protonation site of thiophene is also found to be the α carbon atom on the ring (see eq 14). The most positive (cationic) atom in the protonated thiophene is the sulfur atom (15.529). It appears likely that the water oxygen approaches it through Coulombic attraction. However, the S···O binding energy (7 kcal/mol, STO-3G) is calculated to be much smaller than the hydrogen-bond energy of (14) (15 kcal/mol, STO-3G). The exchange repulsion between O and S atoms lessens the binding energy.

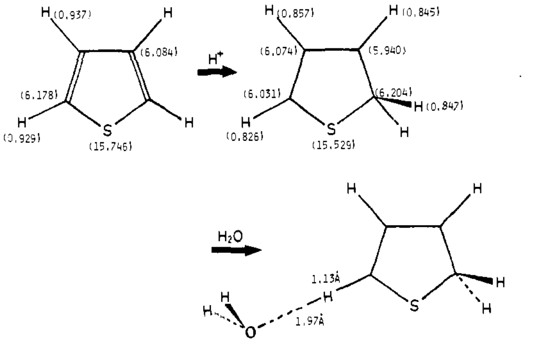

(14)

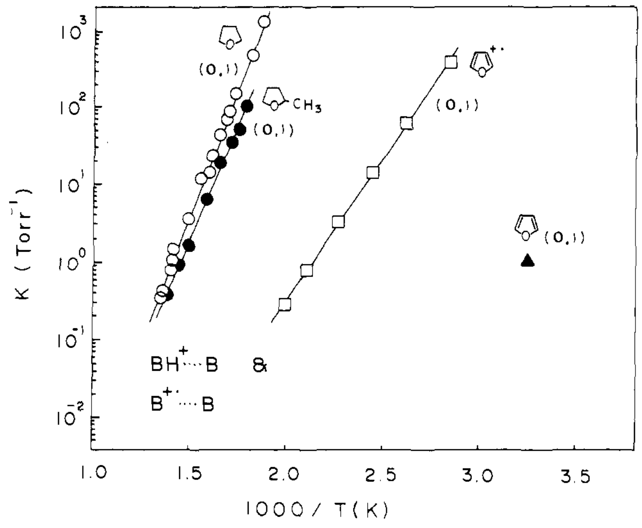

Figure 4. van't Hoff plots for the clustering reactions of protonated and radical cations for tetrahydrofuran (C_4H_8O), 2-methyltetrahydrofuran ($C_5H_{10}O$), and furan (C_4H_4O): (○) $C_4H_8OH^+(C_4H_8O)_{n-1} + C_4H_8O = C_4H_8OH^+(C_4H_8O)_n$, (●) $C_5H_{10}OH^+(C_5H_{10}O)_{n-1} + C_5H_{10}O = C_5H_{10}OH^+(C_5H_{10}O)_n$, (□) $C_4H_4O^{\cdot+}(C_4H_4O)_{n-1} + C_4H_4O = C_4H_4O^{\cdot+}(C_4H_4O)_n$, (▲) $C_4H_5O^+(C_4H_4O)_{n-1} + C_4H_4O = C_4H_5O^+(C_4H_4O)_n$. The reaction designated by ▲ with n = 1 is not in equilibrium at room temperature. The deviation from the equilibria becomes more serious at higher temperature. The equilibrium constant shown in the figure is calculated from the ion intensities of $C_4H_5O^+$ and $C_4H_5O^+(C_4H_4O)$ right after the electron pulse. The value gives only the upper limit of the equilibrium constant.

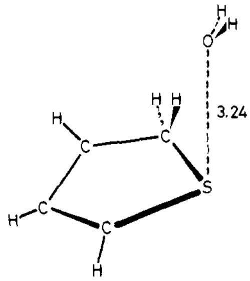

The bond energies of the hydrated clusters of radical cations for furan, pyrrole, and thiophene are slightly lower than those of corresponding protonated bases. Since bonds of hydrated cluster ions are mainly electrostatic, the bond energies give an approximate scale of the positive charge availabilities on the positive sites of cations. The lower bond energies for hydrated radical cations than those for protonated bases suggest that less positive charges are available on the positive sites for radical cations than for protonated bases. This may be due to the well-dispersed positive charges in the radical cations since radical cations still maintain the aromaticities. In fact, the STO-3G UHF MO calculation with geometry optimization demonstrates that the protons for the clustering in the radical cations for furan and thiophene are less acidic than those in the protonated species. The discrepancy observed for pyrrole may be due to either computational deficiency or experimental error.

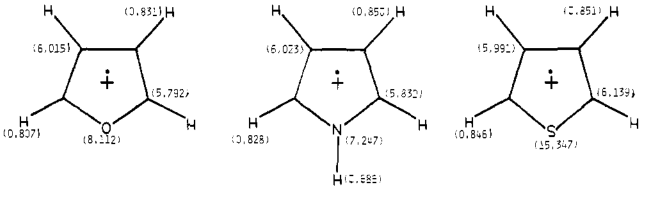

2. Clustering Reactions of Protonated and Radical Cations of Heterocyclic Compounds. Figures 4–6 show van't Hoff plots for the clustering reactions 3 and 4 for B = tetrahydrofuran, pyrrolidine, tetrahydrothiophene, furan, pyrrole, and thiophene. Thermochemical data calculated from the van't Hoff plots are summarized in Tables IV and V.

There is a sudden decrease in the values of $-\Delta H^\circ_{n-1,n}$ between n = 1 and 2 for tetrahydrofuran. This is due to the formation

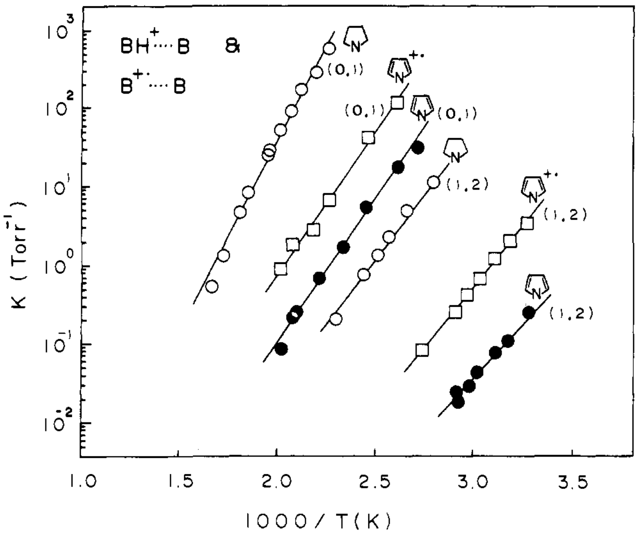

Figure 5. van't Hoff plots for the clustering reactions of protonated and radical cations for both pyrrolidine (C_4H_8NH) and pyrrole (C_4H_4NH): (○) $C_4H_8NH_2^+(C_4H_8NH)_{n-1} + C_4H_8NH = C_4H_8NH_2^+(C_4H_8NH)_n$, (●) $C_4H_5NH^+(C_4H_4NH)_{n-1} + C_4H_4NH = C_4H_5NH^+(C_4H_4NH)_n$, (□) $C_4H_4NH^{\cdot+}(C_4H_4NH)_{n-1} + C_4H_4NH = C_4H_4NH^{\cdot+}(C_4H_4NH)_n$.

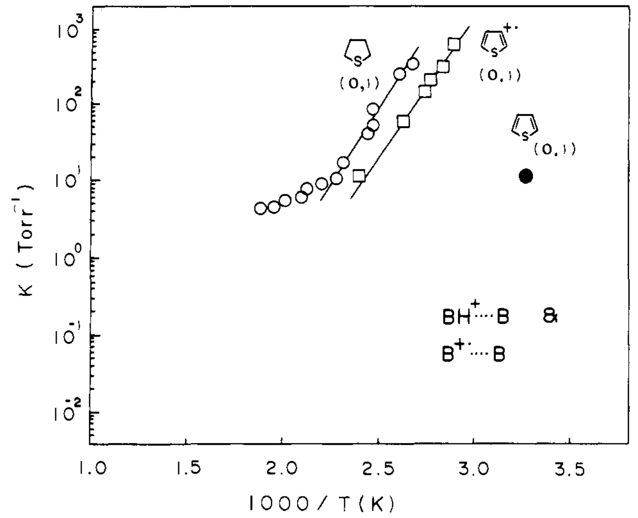

Figure 6. van't Hoff plots for the clustering reactions of protonated and radical cations for tetrahydrothiophene (C_4H_8S) and thiophene (C_4H_4S): (○) $C_4H_8SH^+(C_4H_8S)_{n-1} + C_4H_8S = C_4H_8SH^+(C_4H_8S)_n$, (□) $C_4H_4S^{\cdot+}(C_4H_4S)_{n-1} + C_4H_4S = C_4H_4S^{\cdot+}(C_4H_4S)_n$, (●) $C_4H_5S^+(C_4H_4S)_{n-1} + C_4H_4S = C_4H_5S^+(C_4H_4S)_n$. The equilibria for the reaction designated by ● with $n = 1$ could not be established owing to the presence of impurities. The equilibrium constant shown in the figure is calculated from the ion intensities of $C_4H_5S^+$ and $C_4H_5S^+(C_4H_4S)$ right after the electron pulse. The value gives only the upper limit of the equilibrium constant.

of the first filled-shell structure with $n = 1$ (i.e., $C_4H_8OH^+\cdots OH_8C_4$). The second C_4H_8O molecule interacts with $C_4H_8OH^+(C_4H_8O)$ only weakly from outside of the filled shell.

For pyrrolidine, a smaller decrease in the $-\Delta H°_{n-1,n}$ value between $n = 1$ and 2 is observed. The protonated pyrrolidine has two protic hydrogens and thus it can accommodate two ligand C_4H_8NH molecules to form the first filled-shell structure $C_4H_8NH_2^+(C_4H_8NH)_2$.

The clustering reactions 3 with $n = 1$ for tetrahydrothiophene was found to be somewhat peculiar. The equilibria for reaction 3 with $n = 1$ could be observed below 100 °C. When the ion source temperature is raised above 100 °C, the decay of the proton-held dimer cation $C_4H_8SH^+(C_4H_8S)$ becomes slower than that of the $C_4H_8SH^+$ ion, and proton-held dimer cation persists to exist at higher temperatures. The van't Hoff plots of the apparent equilibrium constants, which are calculated from the ion intensities right after the ionizing electron pulse, deviate from the straight line as shown in Figure 6. We think that this is due to the formation of a more stable ion whose m/z is equal to that of $C_4H_8SH^+(C_4H_8S)$ through the thermal decomposition of the C_4H_8S sample.

Table IV. Thermochemical Data for the Clustering Reactions of Protonated Bases BH^+, $BH^+(B)_{n-1} + B = BH^+(B)_n$[a]

B	(0, 1)		(1, 2)	
	$-\Delta H°$	$-\Delta S°$	$-\Delta H°$	$-\Delta S°$
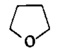	29.9[b] 32.6[c] 32.9[d]	29.1[b] 32.2[c]	7.6	(18)[f]
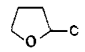	27.4[b]	26.5[b]		
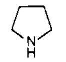	22.3	23.8	15.3	24.3
	16.9	21.0	7.9	(18)[f]
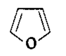	<10			
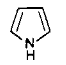	16.8	24.7	12.3	30.4
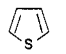	<11.5			
	11.0[e]	24[e]		

[a] $-\Delta H°$ in kcal/mol, $-\Delta S°$ in cal/deg·mol, standard state 1 atm. [b] Reference 14. [c] Reference 2. [d] Reference 1. [e] Reference 17. [f] Entropy value assumed.

Table V. Thermochemical Data for the Clustering Reactions of Radical Cations $B^{\cdot+}$, $B^{\cdot+}(B)_{n-1} + B = B^{\cdot+}(B)_n$[a]

B^+	(0, 1)		(1, 2)	
	$-\Delta H°$	$-\Delta S°$	$-\Delta H°$	$-\Delta S°$
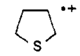 $^{\cdot+}$	>16.9		7.8	(18)[c]
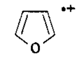 $^{\cdot+}$	17.2	23.7	<7	
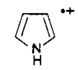 $^{\cdot+}$	16.5	20.3	13.8	29.2
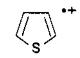 $^{\cdot+}$	16.9	23.1	<7.5	
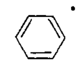 $^{\cdot+}$	17.0[b]	27[b]		

[a] $-\Delta H°$ in kcal/mol, $-\Delta S°$ in cal/deg·mol, standard state 1 atm. [b] Reference 17. [c] Entropy value assumed.

The measurements for the equilibria for the clustering reaction 4 of the radical cation of tetrahydrothiophene with $n = 1$ were not performed since the thermal decomposition of the C_4H_8S sample was anticipated above 100 °C. Since the intensity of the cluster $C_4H_8S^{\cdot+}(C_4H_8S)$ is much stronger than that of $C_4H_8S^{\cdot+}$ at ~100 °C under experimental conditions similar to the measurements of reaction 3, the bond energy of the cluster $C_4H_8S^{\cdot+}\cdots C_4H_8S$ may be much larger than that of the cluster $C_4H_8SH^+\cdots C_4H_8S$ (16.9 kcal/mol).

The equilibria of reaction 3 with $n = 1$ for furan were not established owing to the reactive loss of the $C_4H_5O^+$ ion (see section 3.B). Since the cluster ion $C_4H_5O^+(C_4H_4O)$ is contaminated by the condensation product whose m/z is equal to that of $C_4H_5O^+(C_4H_4O)$, the bond energy of the cluster $C_4H_5O^+(C_4H_4O)$ could only be estimated to be lower than 10 kcal/mol. The equilibria for reaction 3 with $n = 1$ for thiophene could not be established because of the slower decay of the $C_4H_5S^+(C_4H_4S)$ ion compared to that of the $C_4H_5S^+$ ion. This is likely to be due to the contamination of the $C_4H_5S^+(C_4H_4S)$ ion with impurity ions whose m/z is equal to that of

$C_4H_5S^+(C_4H_4S)$ since the inequilibria became more prominent at lower temperatures. The bond energy of the cluster $C_4H_5S^+(C_4H_4S)$ could only be estimated to be less than 11.5 kcal/mol. The estimated bond energies of the proton-held dimer cations for furan and thiophene are much lower than those for tetrahydrofuran and tetrahydrothiophene. This could be further evidence that the heteroatoms are not the most favorable protonation sites for furan and thiophene.

Contrary to the cases for furan and thiophene, the equilibria for reaction 3 with $n = 1$ and 2 could be observed for pyrrole. As in the case of hydration reactions of $C_4H_5NH^+$, the first ligand C_4H_4NH may attack the H atom of the N–H bond of $C_4H_5NH^+$.

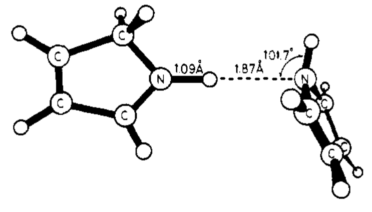

The bond energies of the radical-cation dimers $(B)_2^{\bullet+}$ for furan and thiophene are much larger than those of the proton-held dimer cations for corresponding bases. A similar finding is also obtained for benzene[17] (see Tables III and IV). These findings are in contrast to the fact that the bond energies of $B^{\bullet+}(H_2O)$ are smaller than those of $BH^+(H_2O)$ for furan and thiophene, respectively. Since the radical cations of these compounds maintain the aromaticity, the positive charge is well dispersed through the rings. Such radical cations of diffused positive charges would form bonds with parent aromatic bases through ion-quadrupole interactions; i.e., the radical-cation dimers $(B)_2^{\bullet+}$ may have slippery stack structures. The sudden decrease in the values between $-\Delta H^\circ_{0,1}$ and $-\Delta H^\circ_{1,2}$ found for these compounds also indicates that the bonds in $(B)_2^{\bullet+}$ are not purely electrostatic but have considerable covalent nature. It is known that once the semicovalent bond is formed in the cluster, there appears a sudden decrease in the bond energy of the cluster ion with one more ligand molecule.[18] Some discussion will be given in section 3.B below.

Contrary to the cases for furan and thiophene, equilibria concerning radical-cation clusters $C_4H_4NH^{\bullet+}(C_4H_4NH)_n$ with $n = 1$ and also 2 could be observed. The decrease in the $-\Delta H^\circ_{n-1,n}$ values between $n = 1$ and 2 are only modest. This suggests that the bond of the cluster $C_4H_4NH^{\bullet+}$ (C_4H_4NH) is mainly electrostatic.

3. Clustering Reactions with Covalent Bond Formation. In the previous section, thermochemical data which are incompatible with the mechanism of hydrogen-bond formation are found. Covalency caused by the charge-transfer (CT) interaction should be involved in some clustering reactions. Prior to this analysis, the reason why the carbon is protonated in the conjugated heterocyclic compounds is stated.

A. Protonation to the Furan. The protonation site is predictable by the shape of the highest occupied molecular orbital (HOMO) of furan. It is found that the orbital extension is largest at the α carbon. Thus, the frontier-orbital theory indicates correctly the α protonation in spite of the fact that the α carbon is most cationic. The oxygen protonation is most unfavorable, which is in accord with the computed data.[19] This is because the HOMO is antisymmetric with respect to the *Y–Z* plane and has no component on the oxygen. This HOMO is entirely the same as that in butadiene as is described below. Three occupied π MO's of furan are composed of butadiene, two occupied MO's, and the oxygen p_π atomic orbital (AO). The HOMO of butadiene (B) is antisymmetric and cannot mix the oxygen p_π AO. Thus, the protonation pattern, α-protonation, for the conjugated heterocyclic compounds is quite different from that, heteroatom-protonation, for the saturated one.

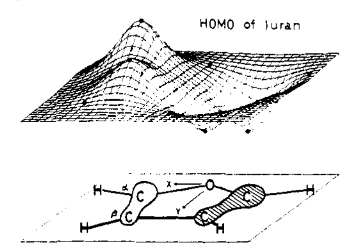

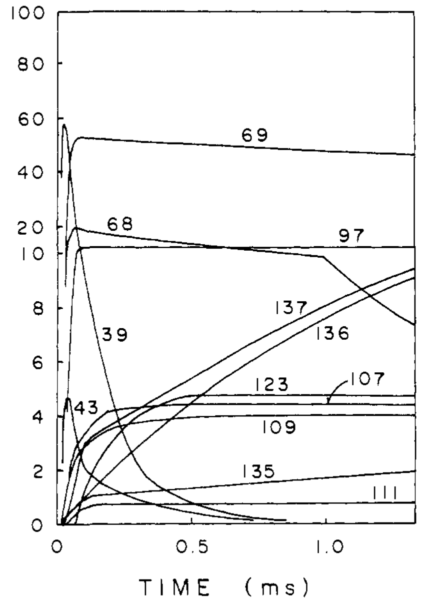

Figure 7. Positive ions observed in a gas mixture containing 4.7 torr of CH_4, 0.68 torr of CS_2, and 0.15 torr of C_4H_4O: mass 39, $C_3H_3^+$; mass 43, $C_3H_7^+$; mass 68, $C_4H_4O^{\bullet+}$; mass 69, $C_4H_5O^+$; mass 97, $C_2H_5^+(C_4H_4O)$; mass 107, $C_3H_3^+(C_4H_4O)$; mass 109, $C_3H_5^+(C_4H_4O)$; mass 111, $C_3H_7^+(C_4H_4O)$; mass 123, probably $C_3H_3O^+(C_4H_4O)$; mass 135, probably $C_4H_3O^+(C_4H_4O)$; mass 136, $C_4H_4O^{\bullet+}$ (C_4H_4O); mass 137, $C_4H_5O^+(C_4H_4O)$. The $C_3H_3^+$ ion is the major product ion from the ion molecule reactions of furan. The precursor ions for this ion were not determined. The decrease in the $C_3H_3^+$ ion is partly accounted for by the increase in the $C_3H_3^+(C_4H_4O)$ ion. The major product ions from the ion/molecule reactions of $C_3H_3^+$ could not be determined.

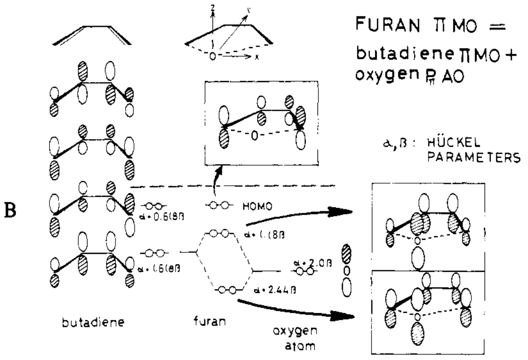

B. Condensation Reactions of Protonated and Radical Cations of Furan. In the temperature range 30–150 °C, the equilibria for reaction 4 for furan could be observed. However, the decay of $(C_4H_4O)_2^{\bullet+}$ becomes slower than that of $C_4H_4O^{\bullet+}$ above 150 °C. The observed slower decay of $(C_4H_4O)_2^{\bullet+}$ should not be due to an impurity since it is only observed at higher temperatures. In the case of the protonated furan, the $C_4H_5O^+(C_4H_4O)$ ion was found to decay slower than the $C_4H_5O^+$ ion already at room temperature.

Figure 7 shows the normalized ion intensities for ions observed after the electron pulse ionization in a gas mixture containing 4.7 torr of CH_4, 0.68 torr of CS_2, and 0.15 torr of C_4H_4O. The gradual decrease in the intensities observed for of $C_4H_4O^{\bullet+}$ and

---

(17) Meot-Ner, M.; Hamlet, P.; Hunter, E. P.; Field, F. H. *J. Am. Chem. Soc.* **1978**, *100*, 5466.

(18) Hiraoka, K.; Shoda, T.; Morise, K.; Yamabe, S.; Kawai, E.; Hirao, K. *J. Chem. Phys.* **1986**, *84*, 2091.

(19) Nguyen, M. T.; Hegarty, A. F.; Ha, T-K; De Mare, G. R. *J. Chem. Soc., Perkin Trans. 2* **1986**, 147.

$C_4H_5O^+$ is accounted for by the increase in those of $(C_4H_4O)_2^{\bullet+}$ and $C_4H_5O^+(C_4H_4O)$, respectively. The occurrence of the condensation reactions of $C_4H_4O^{\bullet+}$ and $C_4H_5O^+$ with a furan molecule is evident. The growth rates of both $(C_4H_4O)_2^{\bullet+}$ and $C_4H_5O^+(C_4H_4O)$ ions increase with temperature up to ~250 °C. The increase in rates of reactions at higher temperatures indicates that the reactions have some energy barrier. Above 250 °C, the growth rates start to decrease and the ions $(C_4H_4O)_2^{\bullet+}$ and $C_4H_5O^+(C_4H_4O)$ could not be detected at ~330 °C under the present experimental conditions. Apparently, finite lifetimes for the intermediate complexes are necessary for these condensation reactions.

It is known that furan condenses in the liquid phase by a Diels–Alder (DA) reaction:

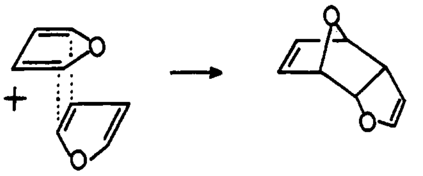

The condensation reactions observed for protonated and radical cations of furan may also be interpreted as the DA reactions. The protonated furan may play a role as an electron acceptor, and accordingly the lowest unoccupied MO (LUMO) is the target for the CT from HOMO of furan. To get the maximum CT, i.e., the HOMO–LUMO overlap, the following stack approach is the best one.

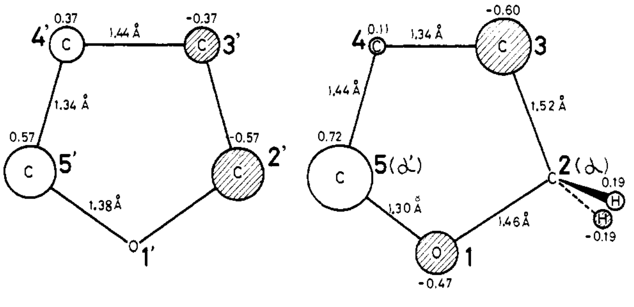

HOMO OF FURAN LUMO OF PROTONATED FURAN

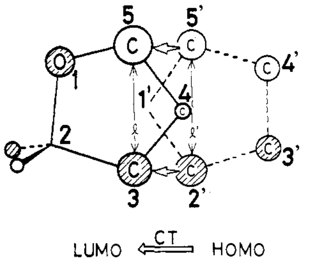

This approach is favorable, also because the $C_3 \cdots C_5$ distance, l = 2.23 Å, is almost the same as the $C_{2'} \cdots C_{5'}$ distance, l' = 2.18 Å. For the DA-type condensation, no significant geometric distortion of furan and protonated furan is needed except for the puckering of the ring. Indeed, the optimized structure of the DA adduct is obtained by the STO-3G MO optimization.

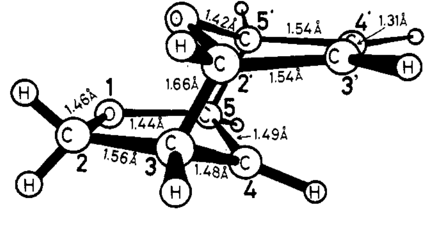

The release of the furan HOMO electron density leads to the elongation (1.34 → 1.54 Å) of $C_{2'}$–$C_{3'}$ and $C_{4'}$–$C_{5'}$ bonds and the shortening (1.44 → 1.31 Å) of the $C_{3'}$–$C_{4'}$ bond, respectively. The decrease of the bonding and antibonding characters of HOMO gives these changes. In the same criterion, the acceptance of the density in the LUMO of the protonated furan elongates the (originally antibonding) O_1–C_5 bond (1.30 → 1.44 Å).

The same discussion holds for the $C_4H_4O^{\bullet+} \cdots C_4H_4O$ cluster. The singly occupied molecular orbital (SOMO) of the furan radical cation has a shape similar to that of the furan HOMO. The (HOMO → SOMO) CT is likely, which leads to the DA-type condensation.

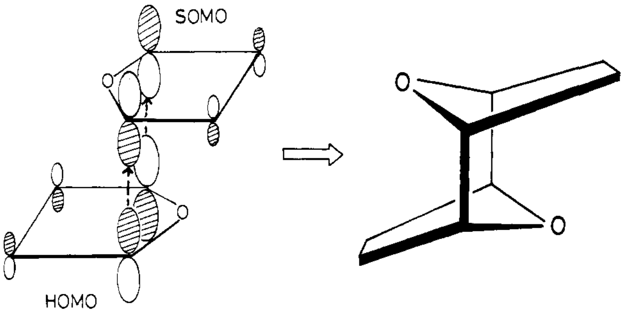

The multi-center condensation reaction is observed for furan but not for pyrrole and thiophene. This may be due to the fact that the aromaticity of furan is the least among these compounds. Actually, the Diels–Alder reactions have not been observed either for benzene or thiophene in the condensed phase. In other words, the p_π AO of heteroatom with small electronegativity can mix well with the carbon p_π AO's, resulting in the delocalization of the frontier orbitals on the heteroatom. The delocalization leads to a decrease in the reactivity of the DA-type condensation.

Concluding Remarks

In this work, the gas-phase clustering and hydration reactions of heterocyclic and radical cation compounds have been investigated. A competition between the hydrogen-bond and covalent-bond formations have been postulated. The hydration reaction is concerned exclusively with the former, and the trend for the thermochemical data is explicable in terms of the acidity of the particular hydrogen except for the protonated tetrahydrothiophene. When such a proton is absent in the cationic species, the (HOMO → SOMO) or (HOMO → LUMO) CT interaction brings about the covalency in the cluster. The five-membered rings have appropriate skeletons to cause the CT interaction effectively and consequently to initiate the DA-type condensation reaction.

Acknowledgment. K.H. thanks for the financial supports of the Grant-in-Aid from the Ministry of Education and of the first Morino Trust for Molecular Science. The authors thank the Data Processing Center of Kyoto University for the allotment of the CPU time of the FACOM M-382 computer. Thanks are also due to the Institute for Molecular Science for our use of the HITAC S-810 computer. Assistance with MO calculations by Mr. Koichi Shimode is gratefully acknowledged.

Registry No. $(C_4H_4O)_2^{\bullet+}$, 110682-33-2; $H^+(C_4H_4O)$, 110661-92-2; $C_4H_8O{\cdot}H^+$, 27659-93-4; $C_4H_7OCH_3{\cdot}H^+$, 69798-80-7; $C_4H_8NH{\cdot}H^+$, 55526-39-1; $C_4H_8S{\cdot}H^+$, 27659-96-7; $C_4H_4O{\cdot}H^+$, 64067-71-6; $C_4H_4NH{\cdot}H^+$, 35745-44-9; $C_4H_4S{\cdot}H^+$, 52165-55-6; C_4H_8O, 109-99-9; $C_4H_7OCH_3$, 96-47-9; C_4H_8NH, 123-75-1; C_4H_8S, 110-01-0; C_4H_4O, 110-00-9; C_4H_4NH, 109-97-7; C_4H_4S, 110-02-1; $C_4H_8S^{\bullet+}$, 87867-43-4; $C_4H_4O^{\bullet+}$, 66429-00-3; $C_4H_4NH^{\bullet+}$, 34468-30-9; $C_4H_4S^{\bullet+}$, 34480-70-1; C_6H_6, 71-43-2; $C_6H_6{\cdot}H^+$, 38815-08-6; $C_6H_6^{\bullet+}$, 34504-50-2; H_2O, 7732-18-5; $CH_2{=}CHCH{=}CH_2$, 106-99-0.